

Optical gain properties in a coherently prepared four-level cold atomic system

Yan Xue, Gang Wang, Jin-Hui Wu, and Jin-Yue Gao*

College of Physics, Jilin University, Changchun 130023, People's Republic of China
and Key Laboratory of Coherent Light, Atomic and Molecular Spectroscopy, Educational Ministry of China, Changchun, People's Republic of China

(Received 7 March 2007; revised manuscript received 24 April 2007; published 28 June 2007)

We analyze the optical gain property of a probe pulse in a four-level system of ultracold ^{87}Rb atoms prepared via a stimulated Raman adiabatic passage type process. During the process of preparation, most population is transferred from the ground state to the highest excited state by two driving pulses in the counterintuitive order. Thus population inversion can be achieved between the highest state and a lower-lying state in a suitable period of time, which then allows very large gain for the probe pulse applied after the driving pulses. In particular, we investigate in detail the influence of several interaction parameters of interest on the probe gain via numerical simulation and qualitative analysis.

DOI: [10.1103/PhysRevA.75.063832](https://doi.org/10.1103/PhysRevA.75.063832)

PACS number(s): 42.50.Gy, 42.50.Hz

I. INTRODUCTION

Coherent excitation has become a standard tool in modern atomic, molecular, and optical physics [1]. One of the effective coherent excitation techniques is known as stimulated Raman adiabatic passage (STIRAP) [2–4], which is usually implemented in the Λ system with intriguing counterintuitive features. Compared with other approaches, such as the application of π pulses [5,6] and that of chirped pulses [7–9], STIRAP is a technique for complete population transfer between stable quantum levels which offers the advantage of significant robustness with respect to variations in laser intensity, timing, and other excitation parameters. This technique has aroused such interesting applications as optical digital logic [10–12], quantum information processing [13,14], and nonlinear dynamics [15,16].

Recently, significant attention has been focused on coherent population transfer in the ladder system of different atoms and molecules. In principle, STIRAP can be implemented without difficulties in the ladder system if the pulse duration is shorter than the lifetime of the highest state. A complete analysis of the excited state population as a function of various interaction parameters in a ^{87}Rb quantum ladder was reported by Camp *et al.* [17]. The control of population flow in molecular ladders was also discussed in detail by two different groups [18,19]. The evidence of efficient coherent population transfer via STIRAP-like processes has already been demonstrated experimentally in ladders of rubidium atoms [20] and Na_2 molecules [21]. From these earlier works, one can see that about 90% population in the ground state can be transferred to the highest state via STIRAP-like processes.

In this paper, we discuss how to achieve very large optical gain for the probe pulse in a four-level double-ladder system via coherent population transfer. Since most atoms can be pumped to the highest state via a STIRAP-like process in one ladder, population inversion is expected to exist between the highest state and the middle state in another ladder. Thus

one can obtain remarkable optical gain on this population-inversed transition in case that a probe pulse is input at a suitable time delay. The aim of this work is to study in detail the optical gain as a function of various interaction parameters through numerically solving the coupled Maxwell-Bloch equations.

II. MODEL AND DENSITY-MATRIX

We show the diagram of our considered four-level system relevant to ^{87}Rb atoms in Fig. 1(a). Levels $|1\rangle$, $|2\rangle$, $|3\rangle$, and $|4\rangle$, respectively, correspond to states $^5S_{1/2}$, $^5P_{3/2}$, $^6S_{1/2}$, and $^5P_{1/2}$ of ^{87}Rb atoms. The pump laser Ω_1 is detuned from the $^5S_{1/2}$ - $^5P_{3/2}$ transition by δ_1 , the Stokes laser Ω_2 is detuned from the $^5P_{3/2}$ - $^6S_{1/2}$ transition by δ_2 , while the probe laser Ω_p is detuned from the $^5P_{1/2}$ - $^6S_{1/2}$ transition by δ_p . Note that, to perform efficient STIRAP processes, we should require in

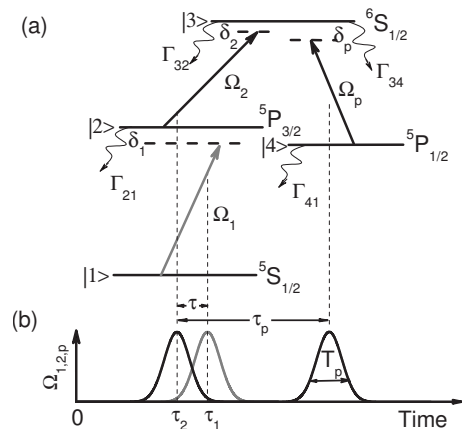


FIG. 1. (a) Schematic diagram of a four-level ^{87}Rb atom system. Levels $|1\rangle$, $|2\rangle$, $|3\rangle$, and $|4\rangle$, respectively, correspond to energy levels of ^{87}Rb atom $^5S_{1/2}$, $^5P_{3/2}$, $^6S_{1/2}$, and $^5P_{1/2}$. Level $|1\rangle$ and $|2\rangle$ are coupled by the Ω_1 pulse, and level $|2\rangle$ and $|3\rangle$ are coupled by the Ω_2 pulse. The probe pulse Ω_p is applied to the transition $|4\rangle \rightarrow |3\rangle$. (b) Pulse sequence applied in the system. The pump pulse Ω_1 and the Stokes pulse Ω_2 are arranged in the counterintuitive order.

*Corresponding author; jygao@mail.jlu.edu.cn

the following the two-photon resonance condition $\delta_1 + \delta_2 = 0$. Γ_{ij} denotes the spontaneous decay rate from level $|i\rangle$ to level $|j\rangle$. Here we have $\Gamma_{21} = 38.11$ MHz, $\Gamma_{32} = 7.46$ MHz, $\Gamma_{34} = 14.48$ MHz, and $\Gamma_{41} = 36.10$ MHz [22,23]. It is clear that the lifetime of level $|3\rangle$ is longer than that of level $|4\rangle$, which then follows that the population inversion between levels $|3\rangle$ and $|4\rangle$ can be maintained for a relatively longer time.

In the interaction picture, with the rotating-wave and electric-dipole approximations, the Hamiltonian can be expressed as

$$H_I = \hbar \begin{bmatrix} 0 & -\Omega_1^* & 0 & 0 \\ -\Omega_1 & \delta_1 & -\Omega_2^* & 0 \\ 0 & -\Omega_2 & \delta_1 + \delta_2 & -\Omega_p \\ 0 & 0 & -\Omega_p^* & \delta_1 + \delta_2 - \delta_p \end{bmatrix} \quad (1)$$

with Ω_1 , Ω_2 , and Ω_p being, respectively, Rabi frequencies of the pump, Stokes, and probe fields, while Ω_i^* is the complex conjugate of Ω_i . Concretely, we have $\Omega_1 = d_{12}E_1/2\hbar$, $\Omega_2 = d_{23}E_2/2\hbar$, and $\Omega_p = d_{43}E_p/2\hbar$ with $E_{1,2,p}$ being the involved electric-field amplitudes and d_{mn} the corresponding dipole moments. Then we can describe the quantum dynamics of the four-level atomic system by the Liouville equation,

$$\frac{\partial \rho}{\partial t} = -\frac{i}{\hbar}[H_I, \rho] - \frac{1}{2}\{\Gamma, \rho\}, \quad (2)$$

which should be solved together with the Maxwell equations provided all three fields are pulsed or time dependent, namely

$$\begin{aligned} \frac{\partial \Omega_1}{\partial z} + \frac{1}{c} \frac{\partial \Omega_1}{\partial t} &= i \frac{Nd_{12}^2 \omega_1}{\epsilon_0 \hbar c} \rho_{21}, \\ \frac{\partial \Omega_2}{\partial z} + \frac{1}{c} \frac{\partial \Omega_2}{\partial t} &= i \frac{Nd_{23}^2 \omega_2}{\epsilon_0 \hbar c} \rho_{32}, \\ \frac{\partial \Omega_p}{\partial z} + \frac{1}{c} \frac{\partial \Omega_p}{\partial t} &= i \frac{Nd_{43}^2 \omega_p}{\epsilon_0 \hbar c} \rho_{34}, \end{aligned} \quad (3)$$

where N (typically $10^9 - 10^{11}$ atoms/cm³ for ultracold ⁸⁷Rb atoms in MOT) is the atomic density, ϵ_0 the permittivity of the vacuum, and c the speed of light in vacuum. The space-time evolution of the three laser pulses passing through clouds of ultracold ⁸⁷Rb atoms can be assessed by simultaneously solving Eq. (2) and Eq. (3), which will be numerically examined in several different situations in the next section.

III. NUMERICAL ANALYSIS AND DISCUSSIONS

For the following numerical calculations, all three laser fields are assumed as Gaussian pulses: $\Omega_1(t) = \alpha_1 e^{-(t-\tau_1)^2/T^2}$, $\Omega_2(t) = \alpha_2 e^{-(t-\tau_2)^2/T^2}$, and $\Omega_p(t) = \alpha_p e^{-(t-\tau_2-\tau_p)^2/T_p^2}$ with $\tau_2 = 6T$ and $\alpha_1 = \alpha_2 = 20T^{-1}$. Here the pulse duration $T = 0.04\Gamma_{32}^{-1}$ is assumed within the range of experimental possibilities. For every STIRAP process, the pump and Stokes pulses are arranged in the counterintuitive order. The delay time

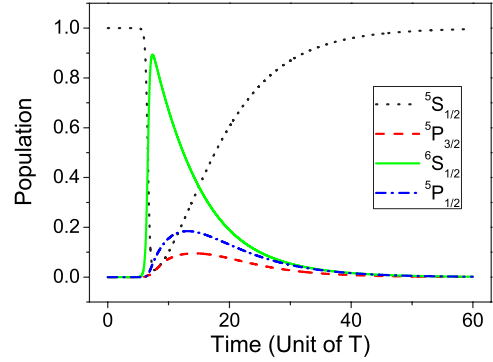


FIG. 2. (Color online) Typical plot of populations versus time when the delay time between the pump and Stokes pulses $\tau = 1.2T$.

of the Stokes pulse relative to the pump pulse is given by $\tau = \tau_1 - \tau_2$, while that of the probe pulse relative to the Stokes pulse is defined by τ_p [see Fig. 1(b)].

We first consider how to obtain large population accumulation at level $|3\rangle$ so that significant probe gain becomes viable. For simplicity, we set $\alpha_{p0} = 0$ to exclude the contribution from the probe field. In agreement with Refs. [17,21], we find from Fig. 2 that more than 80% population can be transferred from level $|1\rangle$ to level $|3\rangle$ in a small span of time when the delay time τ is $1.2T$. The fact that the maximal population at level $|3\rangle$ is about 90% during the STIRAP process is just due to the inevitable spontaneous decay. It is also clear that population inversion exists between levels $|3\rangle$ and $|4\rangle$ in a relatively larger time span, which may be used to amplify the probe pulse arriving after the pump and Stokes pulses. As illustrated in Fig. 3, as large as 50% optical gain is achieved when the probe pulse with $\tau_p = 10T$ goes through a $z = 2$ mm long cloud of ultracold ⁸⁷Rb atoms. Note that our predicted probe gain is much larger than that with or without population inversion reported in Refs. [24–26].

Then, apart from population inversion, are there other contributions, e.g., quantum coherence, on the remarkable probe gain? To answer this question, we resort to the equa-

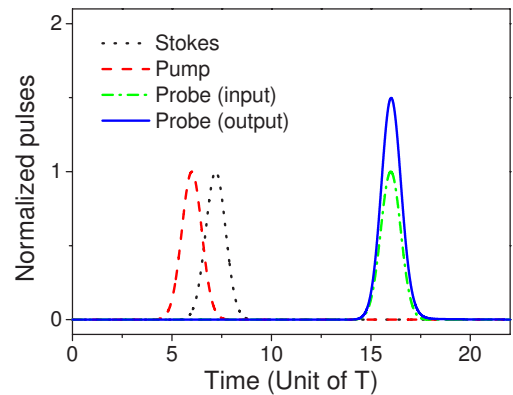


FIG. 3. (Color online) Typical time evolution plot of probe gain. The pulses Ω_1 , Ω_2 , and Ω_p are normalized by α_1 , α_2 , and α_{p0} , respectively. The parameters used here are assumed as $z = 2$ mm, $\alpha_{p0} = 17\Gamma_{32}$, $\tau_p = 10T$, and $T_p = T$. Other parameters are the same as in Fig. 2.

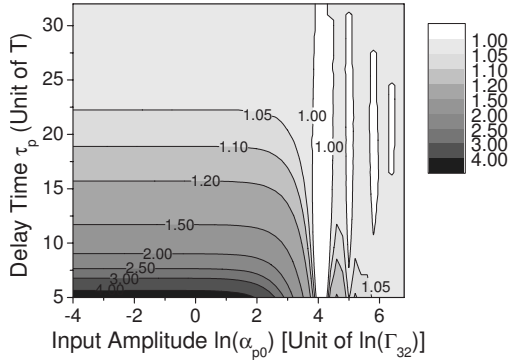


FIG. 4. Maximum probe gain versus the input amplitude α_{p0} and the delay time τ_p . The input amplitude α_{p0} is scaled by Γ_{32} . The parameters used here are assumed as $z=2$ mm and $T_p=T$.

tion of motion for the density matrix element ρ_{34} , whose imaginary part governs the gain property on the probe transition. From Eq. (2), it is straightforward to derive the following equation:

$$\frac{\partial \rho_{34}}{\partial t} = -\frac{1}{2}(\Gamma_{32} + \Gamma_{34} + \Gamma_{41})\rho_{34} + i[-\Omega_2\rho_{24} + \Omega_p(\rho_{33} - \rho_{44})], \quad (4)$$

where $\delta_p=0$ has been considered. In our calculations shown before and later, the Stokes pulse vanishes before the probe pulse is applied, so the contribution of the quantum coherence term $\Omega_2\rho_{24}$ on the probe gain can be reasonably omitted. Therefore, one can conclude that it is the population inversion that essentially determines the probe gain demonstrated in this paper.

Next, we consider how to achieve the largest probe gain by modulating various parameters of the input probe pulse, such as the amplitude α_{p0} , the delay time τ_p , and the duration T_p . As for the probe detuning δ_p , it is obvious that the largest probe gain should correspond to $\delta_p=0$, so all of the following calculations will be implemented for the resonant probe field.

In Fig. 4, we plot the maximal probe gain $\max \Omega_p^2/\alpha_{p0}^2$ versus the amplitude α_{p0} and the delay time τ_p with a fixed duration $T_p=T$ and a fixed length $z=2$ mm. We can see that, for small fixed amplitudes α_{p0} , the probe gain decreases gradually when the delay time τ_p tends to be longer. This result is intuitive because the population difference $\rho_{33}-\rho_{44}$ reduces monotonously after its only peak with the increasing of time. Thus, the later the probe pulse is input, the smaller the maximal probe gain can be obtained. On the other hand, when the delay time τ_p is fixed, the maximal probe gain becomes smaller and smaller with the increasing of amplitude α_{p0} . This is because the number of atoms at level $|3\rangle$ is limited by the atomic density, the medium length, and strengths of the pump and Stokes pulses, and this limited atomic number is not enough for a very strong probe to maintain the same optical gain as that of a relatively weak probe. We further note that the probe pulse may reach the gain saturation when its amplitude is large enough.

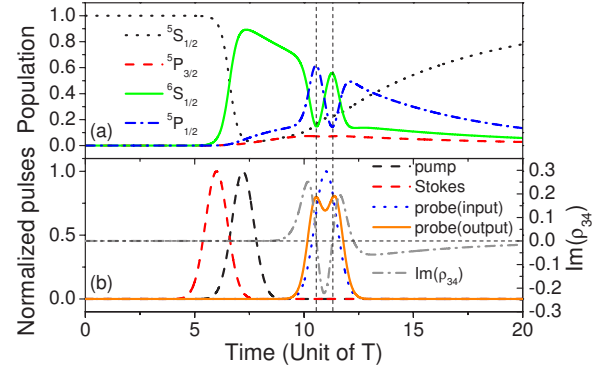


FIG. 5. (Color online) Time evolution plot of populations (a), of variational behavior of probe field and of the density matrix element $\text{Im}(\rho_{34})$ (b). The pulses Ω_1 , Ω_2 , and Ω_p are normalized by α_1 , α_2 , and α_{p0} , respectively. The parameters used here are assumed as $z=2$ mm, $\alpha_{p0}=63\Gamma_{32}$, $\tau_p=5T$, and $T_p=T$.

Figure 4 also shows that, for very strong probe pulses, there exist several regions where the probe pulse is absorbed but not amplified. We can understand this phenomenon by discussing the dynamical process of pulse propagation. As we know, when a probe pulse propagates in a certain gain medium, its rising edge is always amplified before its trailing edge. In our case, if the probe pulse is strong enough, its rising edge amplification may exhaust the population inversion between levels $|3\rangle$ and $|4\rangle$. After the exhaustion of population inversion between levels $|3\rangle$ and $|4\rangle$, it goes without saying that the following population inversion between levels $|3\rangle$ and $|4\rangle$ may be achieved again. In case the probe Rabi frequency is large enough, the probe gain and absorption will occur alternately during the propagation process, which is accompanied by the Rabi oscillation of population between levels $|3\rangle$ and $|4\rangle$.

To have a direct perception on the oscillation dynamics, we plot in Fig. 5 the typical time evolutions of populations at different levels and amplitudes of different pulses. It is clear that the probe gain and absorption are governed by the imaginary part of ρ_{34} (see the dashed-dotted curve), or more precisely, by populations at levels $|3\rangle$ and $|4\rangle$. The rising edge of the probe pulse is amplified first due to the population inversion between levels $|3\rangle$ and $|4\rangle$, during which the population is transferred from level $|3\rangle$ to level $|4\rangle$. When the population at level $|3\rangle$ reaches its minimum, the probe pulse begins to be absorbed and the population is transferred in the opposite direction, i.e., from level $|4\rangle$ to level $|3\rangle$. When the population at level $|3\rangle$ reaches its maximum, the probe pulse begins to be amplified again due to population inversion. As a result, the rising and trailing edges of the probe pulse are amplified while its central part is absorbed. Since the maximal amplitude of the output probe is smaller than that of the input probe [see Fig. 5(b)], we conclude that Rabi oscillation leads to the probe absorption.

Figure 6 shows the effects of α_{p0} and T_p on the maximal probe gain with a fixed delay time $\tau_p=15T$. We can see that, for each fixed pulse duration T_p , the maximal probe gain decreases gradually when the pulse amplitude α_{p0} becomes

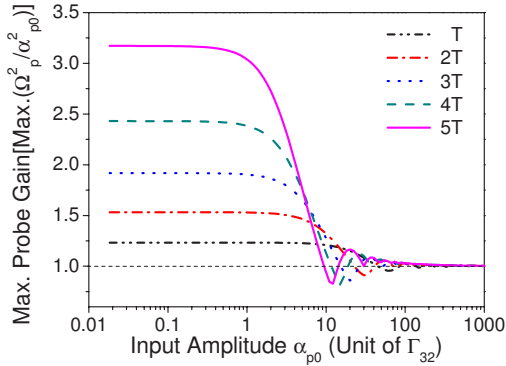


FIG. 6. (Color online) Maximum probe gain versus input amplitude α_{p0} and pulse duration T_p . The input amplitude α_{p0} is scaled by Γ_{32} . The parameters used here are assumed as $z=2$ mm, and $\tau_p=15T$.

larger, which is consistent with Fig. 4. On the other hand, for each fixed pulse amplitude α_{p0} , the maximum probe gain increases gradually when the pulse duration T_p becomes longer. In our case, the pulse duration T_p is approximately the interaction time of the probe field with the medium. Thus the longer the pulse duration T_p is, the more the pumping energy is transferred to the probe pulse so that a larger probe gain can be achieved. This is especially true when the probe pulse is very weak. Due to the limited pumping energy, when the pulse amplitude α_{p0} increases to a certain value, the maximal probe gain begins to decrease and the difference between any two gain curves becomes smaller.

Finally, we discuss something interesting about the atomic density N , which is usually in the range from 3.5×10^9 atoms/cm³ [27] to 2.4×10^{11} atoms/cm³ [28] for ultracold ⁸⁷Rb atoms. In Fig. 7, we trace the maximum probe gain as a function of the atomic density in this realistic range. Our intuition is that a larger atomic density will result in a larger probe gain because more atoms are available to the probe amplification. Figure 7 shows that, however, the probe gain does not monotonously increase with the atomic density and there is a region where the probe gain is reduced. Here the probe pulse is so weak that the Rabi oscillation of population will not occur between levels $|3\rangle$ and $|4\rangle$ in the

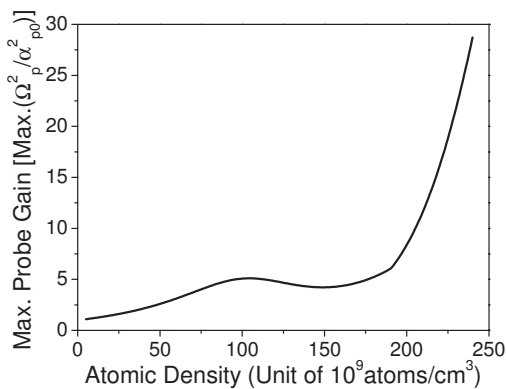


FIG. 7. Probe gain versus atomic density N . The parameters used here are assumed as $\alpha_{p0}=0.01\Gamma_{32}$, $\tau_p=10T$, and $T_p=T$.

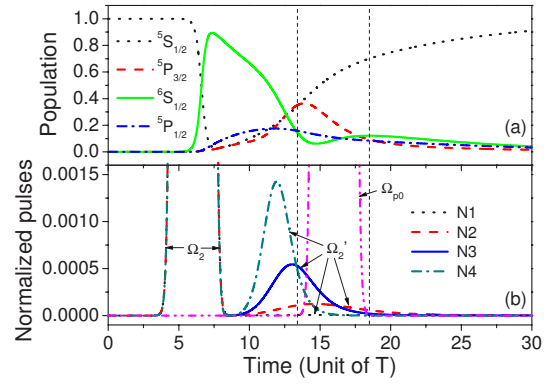


FIG. 8. (Color online) (a) Time evolution plot of populations when the atomic density is considered as 1.5×10^{11} atoms/cm³. (b) Numerical evidence for the generated pulse field Ω'_2 . Here, the atomic density is assumed as $N1=6 \times 10^{10}$ atoms/cm³, $N2=1.05 \times 10^{11}$ atoms/cm³, $N3=1.5 \times 10^{11}$ atoms/cm³, and $N4=2 \times 10^{11}$ atoms/cm³. The pulse fields Ω_2 and Ω'_2 are normalized by α_2 . The parameters used here are assumed as $z=2$ mm, $\alpha_{p0}=0.01\Gamma_{32}$, $\tau_p=10T$, and $T_p=T$.

amplification process. Thus, the reduced gain of a weak probe should be different in physics from the absorption of a strong probe shown in Fig. 4. Since there is also population inversion on transition $|3\rangle \leftrightarrow |2\rangle$ after the STIRAP process, we estimate that the reduced probe gain be related to a generated pulse Ω'_2 resulting from the population transfer from level $|3\rangle$ to level $|2\rangle$. If the generated pulse Ω'_2 is strong and the population transfer from level $|3\rangle$ to level $|2\rangle$ is significant, the population inversion on transition $|3\rangle \leftrightarrow |4\rangle$ will become very small so that the probe gain is remarkably reduced.

To verify our estimation, we plot the typical population evolutions with $N=1.5 \times 10^{11}$ atoms/cm³ in Fig. 8(a) and the amplitudes of relevant pulses obtained with different atomic density in Fig. 8(b). We can see that, with the increasing of N , the generated pulse Ω'_2 becomes stronger and stronger and simultaneously closer and closer to the Stokes pulse Ω_2 . In particular, when the generated pulse is large enough, Rabi oscillation occurs between levels $|3\rangle$ and $|2\rangle$ within the pulse duration of Ω'_2 . As a result, the population at level $|3\rangle$ is less than that at level $|4\rangle$ when the probe pulse is applied, which certainly will lead to the reduced gain. If the medium has a much smaller atomic density, the Rabi oscillation between levels $|3\rangle$ and $|2\rangle$ will not occur because the generated pulse Ω'_2 is too weak. In this case, the probe pulse will be amplified as usual. Conversely, if the medium has a much larger atomic density, population inversion can be achieved again between levels $|3\rangle$ and $|4\rangle$ in the probe pulse duration due to the stronger Rabi oscillation caused by Ω'_2 , so the probe pulse will be amplified again.

IV. SUMMARY

In summary, our quantitative calculation and qualitative analysis show that very large optical gain can be achieved in a coherently prepared four-level system of ultracold ⁸⁷Rb atoms. The dependence of the optical gain on the probe am-

plitude α_{p0} , the probe delay time τ_p , the probe duration T_p , and the atomic density N is studied in detail. The physical mechanism of the probe gain is also discussed. From the numerical results, we find that our predicted probe gain is much larger than those in earlier works. The gain mechanism proposed in this paper shows a significant prospect in the field of short-wavelength light amplification, giant light amplification, and improved lasing efficiency.

ACKNOWLEDGMENTS

The authors would like to thank the support of the National Natural Science Foundation of China under Grants Nos. 10334010 and 10404009; the National Basic Program under Grant No. 2006CB921101; the doctoral program foundation of the Institution of High Education of China; and the Graduate Innovation Laboratory of Jilin University.

-
- [1] B. W. Shore, *The Theory of Coherent Atomic Excitation* (Wiley, New York, 1990).
- [2] K. Bergmann, H. Theuer, and B. W. Shore, *Rev. Mod. Phys.* **70**, 1003 (1998).
- [3] N. V. Vitanov, T. Halfmann, B. W. Shore, and K. Bergmann, *Annu. Rev. Phys. Chem.* **52**, 763 (2001).
- [4] N. V. Vitanov, M. Fleischhauer, B. W. Shore, and K. Bergmann, *Adv. At., Mol., Opt. Phys.* **46**, 55 (2001).
- [5] I. Roos and K. Molmer, *Phys. Rev. A* **69**, 022321 (2004).
- [6] D. Felinto, L. H. Acioli, and S. S. Vianna, *Phys. Rev. A* **70**, 043403 (2004).
- [7] B. Broers, H. B. van Linden van den Heuvell, and L. D. Noordam, *Phys. Rev. Lett.* **69**, 2062 (1992).
- [8] P. Balling, D. J. Maas, and L. D. Noordam, *Phys. Rev. A* **50**, 4276 (1994).
- [9] D. J. Maas, C. W. Rella, P. Antoine, E. S. Toma, and L. D. Noordam, *Phys. Rev. A* **59**, 1374 (1999).
- [10] Z. Kis and F. Renzoni, *Phys. Rev. A* **65**, 032318 (2002).
- [11] C. Y. Ye, V. A. Sautenkov, Y. V. Rostovtsev, and M. O. Scully, *Opt. Lett.* **28**, 2213 (2003).
- [12] F. Remacle and R. D. Levine, *Phys. Rev. A* **73**, 033820 (2006).
- [13] X. Lacour, S. Guerin, N. V. Vitanov, L. P. Yatsenko, and H. R. Jauslin, *Opt. Commun.* **264**, 362 (2006).
- [14] L. M. Duan, J. I. Cirac, and P. Zoller, *Science* **292**, 1695 (2001).
- [15] K. Na and L. E. Reichl, *Phys. Rev. A* **72**, 013402 (2005).
- [16] Xue Yan, He Qiong-Yi, G. C. LaRocca, M. Artoni, Xu Ji-Hua, and Gao Jin-Yue, *Phys. Rev. A* **73**, 013816 (2006).
- [17] H. A. Camp, M. H. Shah, M. L. Trachy, O. L. Weaver, and B. D. DePaola, *Phys. Rev. A* **71**, 053401 (2005).
- [18] M. L. Almazor, O. Dulieu, M. Elbs, E. Tiemann, and F. Masnou-Seeuws, *Eur. Phys. J. D* **5**, 237 (1999).
- [19] L. P. Yatsenko, A. A. Rangelov, N. V. Vitanov, and B. W. Shore, *J. Chem. Phys.* **125**, 014302 (2006).
- [20] W. Süptitz, B. C. Duncan, and P. L. Gould, *J. Opt. Soc. Am. B* **14**, 1001 (1997).
- [21] R. Garcia-Fernandez, A. Ekers, L. P. Yatsenko, N. V. Vitanov, and K. Bergmann, *Phys. Rev. Lett.* **95**, 043001 (2005).
- [22] M. S. Safronova, C. J. Williams, and C. W. Clark, *Phys. Rev. A* **69**, 022509 (2004).
- [23] E. Gomez, F. Baumer, A. D. Lange, G. D. Sprouse, and L. A. Orozco, *Phys. Rev. A* **72**, 012502 (2005).
- [24] J. Kitching and L. Hollberg, *Phys. Rev. A* **59**, 4685 (1999).
- [25] S. R. de Echaniz, A. D. Greentree, A. V. Durrant, D. M. Segal, J. P. Marangos, and J. A. Vaccaro, *Phys. Rev. A* **64**, 055801 (2001).
- [26] H. S. Kang, L. L. Wen, and Y. F. Zhu, *Phys. Rev. A* **68**, 063806 (2003).
- [27] J. Wang, Y. F. Zhu, K. J. Jiang, and M. S. Zhan, *Phys. Rev. A* **68**, 063810 (2003).
- [28] H. S. Kang, G. Hernandez, and Y. F. Zhu, *Phys. Rev. A* **70**, 011801(R) (2004).